Asian Journal of Chemistry; Vol. 30, No. 12 (2018), 2731-2736

ASIAN JOURNAL OF CHEMISTRY

https://doi.org/10.14233/ajchem.2018.21572

Growth and Characterization of Bisthiourea Lithium Sodium Sulphate: A Novel Semiorganic Nonlinear Optical Single Crystals

R. PUNNIYAMOORTHY, R. SUGANTHI, R. MANIMEKALAI and G. PASUPATHI*

PG and Research Department of Physics, A.V.V.M. Sri Pushpam College (Autonomous), Poondi, Thanjavur-613 503, India

*Corresponding author: E-mail: gpasupathi123@gmail.com

Received: 10 July 2018; *Accepted*: 20 September 2018; *Published online*: 31 October 2018; AJC-19139

The semi organic nonlinear optical (NLO) material bisthiourea lithium sodium sulphate (BTLSS) was grown by slow evaporation growth technique. The grown crystal is subjected to single crystal XRD and powder X-ray diffraction with MoKα and CuKα radiation respectively for the determination of unit cell parameters and crystalline nature. The presence of functional groups in BTLSS was identified by FT-IR spectral evaluation. The optical properties of BTLSS have been determined by UV-Vis-NIR spectral analysis and the lower cut off wavelength is 300 nm. The fluorescence study was confirmed that the green emission of BTLSS, which suggests that the grown crystal is properly acceptable for NLO applications. The thermal behaviors of the grown crystals have been investigated by means of TG/DTA analyzer. The mechanical behaviors of the grown crystal were analyzed by Vickers micro hardness tester. Second harmonic generation (SHG) efficiency of the BTLSS was measured by Kurtz and Perry technique. The magnetic property of BTLSS was studied by vibrating sample Magnetometer.

Keywords: Crystal growth, Optical studies, Luminescence, Thermal analysis, Mechanical behavior, Magnetic properties.

INTRODUCTION

Nonlinear optics is playing a prominent role in the development of photonic and optoelectronic technologies. New nonlinear optical (NLO) materials have the main impact on laser technology, optical communication, optical switching, optical data storage and frequency shifting. Second order nonlinear optical materials have currently attracted plenty of attention due to their potential applications on sprouting optoelectronic technologies [1-3]. Inorganic NLO materials have notable mechanical strength, thermal stability and good transmittance. However modest optical non-linearity appear because of their lack of prolonged π-electron dislocation. Purely organic NLO materials have high non-linearity compared to inorganic materials but short optical transparency, poor thermal and mechanical strength and low laser damage threshold. Hence, the research is inspired on semiorganic NLO material in an effort to attain superior NLO crystal uniting the advantages of organic and inorganic materials. The semiorganic NLO materials were attracting much attention due to highest optical nonlinearity, chemical flexibility with the high mechanical and thermal stability [4-6].

In recent years, the NLO properties of semiorganic complex merchandise of thiourea have attracted as a high-quality due to these metal-organic complexes combine the high optical nonlinearity with the physical ruggedness of inorganic materials. Thiourea molecule is a motivating inorganic matrix modifier because of its enormous dipole moment and its capability to form a widespread network of hydrogen bonds. The centrosymmetric of a good ligand thiourea molecule when coordinated with metal ions, it yields non-centrosymmetric complexes to exhibit second harmonic generation (SHG) activity [7-9]. Several metal-organic complexes of thiourea such as bisthiourea cadmium acetate (BTCA), bisthiourea zinc formate (BTZF), tristhiourea zinc cadmium sulphate (TTZCS), tristhiourea magnesium zinc sulphate (TTMZS), bisthiourea sodium zinc sulphate (BTSZS), bisthiourea lithium potassium sulphate (BTLKS) have already been studied [10-15]. In the present investigation, thiourea combines with lithium sulphate and sodium sulphate becomes more NLO active. Motivated by the above considerations, it is aimed to grow bisthiourea lithium sodium sulphate (BTLSS) new semiorganic single crystal by slow evaporation technique. The crystal has been investigated

by different characterization techniques, such as FTIR, single crystal XRD, powder XRD, optical, thermal, mechanical and magnetic properties and second harmonic generation (SHG).

EXPERIMENTAL

Crystal growth: Bisthiourea lithium sodium sulphate (BTLSS) was synthesized by reacting thiourea (AR grade), lithium sulphate (AR grade) and sodium sulphate (AR grade) in the molar ratio of 2:1:1 in double distilled water [15]. The chemical reaction is given below:

$$2[CS(NH_2)_2] + Li_2SO_4{:}H_2O + Na_2SO_4 \longrightarrow 2[Li\ Na\ (CS(NH_2)_2]SO_4 + H_2O$$

The synthesized salt was purified by repeated recrystallization process. The growth of BTLSS crystal was attained by taking the exact amount of salt dissolved in double distilled water by continuous stirring for 3 h. The solution was filtered twice using the Whatman filter paper and growth vessel was covered with a polythene paper. Hence, few holes were made in the polythene paper for slow evaporation at room temperature (30 ºC) and the solution was left undisturbed. The good quality transparent BTLSS crystal of size 13 mm × 7 mm × 2 mm was harvested in 25 days (Fig. 1).

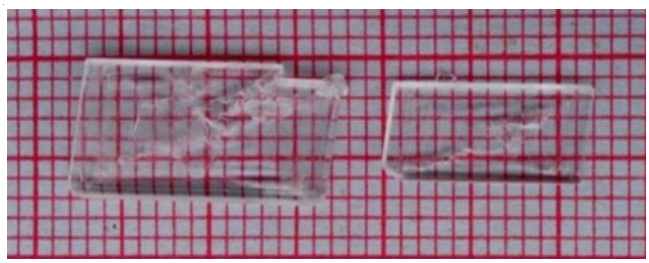

Fig. 1. As grown BTLSS single crystal

RESULTS AND DISCUSSION

Single crystal XRD analysis: Single crystal X-ray diffraction is a non-destructive analytical method which provides the unit cell dimensions. The grown BTLSS crystal became subjected to single crystal X-ray diffraction studies using an ENRAF NONIUS CAD 4 diffractometer with MoKα radiation (λ = 0.71073 Å) at room temperature. The observed lattice parameters are a = 17.825 Å; b = 8.177 Å; c = 6.235 Å and α = β = γ = 90º. The volume of the unit cell is found to be V = 908.89 Å^3. Hence, the grown crystal belongs to orthorhombic crystal system with non-centrosymmetric space group P$n2_1a$.

Powder XRD analysis: The uniform fine powder of grown crystal was subjected to powder X-ray diffractometer analysis using XPERT-PRO diffractometer system with CuKα (λ = 1.54060 Å) radiation. The sample in the form of a thin film was scanned over the range 10-80º at a scan rate of 2º/min. The powder XRD pattern of BTLSS is shown in Fig. 2. The miller indices are calculated and the Bragg′s peaks were indexed. The (hkl) planes fulfill the general reflection conditions of space group identified from the structure determination of the crystal. The experimental data was found to agree well with the calculated (d) values and sharp peaks indicate the crystallinity nature of grown crystal.

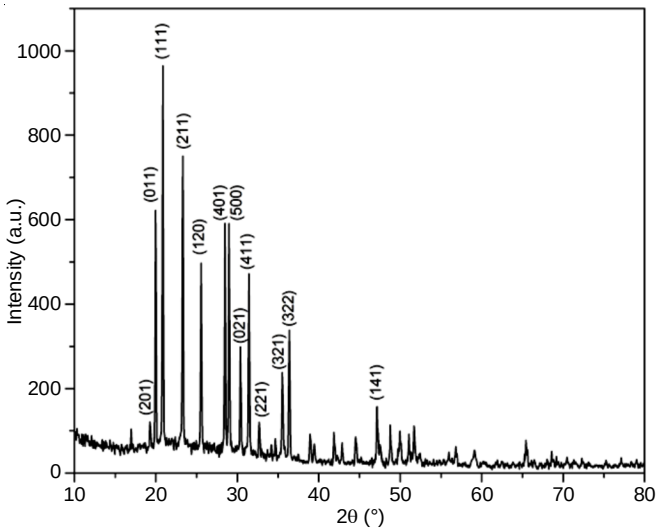

Fig. 2. Powder XRD pattern of BTLSS

FTIR analysis: The FT-IR spectral analysis of BTLSS crystal was carried out between 4000 and 400 cm^{-1} using Perkin Elmer RX1 spectrometer by KBr pellet technique. The FT-IR spectroscopy is effectively used to identify the functional groups and provides more information about the molecular structure of synthesized compounds. The recorded FT-IR spectrum of BTLSS compound is shown in Fig. 3. In the high frequency region, sharp intense peaks were observed at 3377 and 3166 cm^{-1} corresponds to asymmetric and symmetric stretching vibration modes of NH_2 of thiourea molecule [13]. The peak at 1592 cm^{-1} is due to the bending absorption of NH_2. The C=N symmetric and asymmetric stretching vibrations occurred at 1089 and 1468 cm^{-1}, respectively. The sharp peaks appeared at 741 and 1427 cm^{-1} is due to C=S symmetric and asymmetric stretching vibration, respectively. The prominent SO_4 stretching frequencies were assigned at 1628, 1121, 719 and 618 cm^{-1}. The peaks at 635 and 485 cm^{-1} is assigned to symmetric and asymmetric NCS bending [16,17]. From FT-IR spectrum, the presence of functional groups and the coordination ligands of BTLSS were ascertained. The assignment of functional groups is given and compared with the similar compound in Table-1.

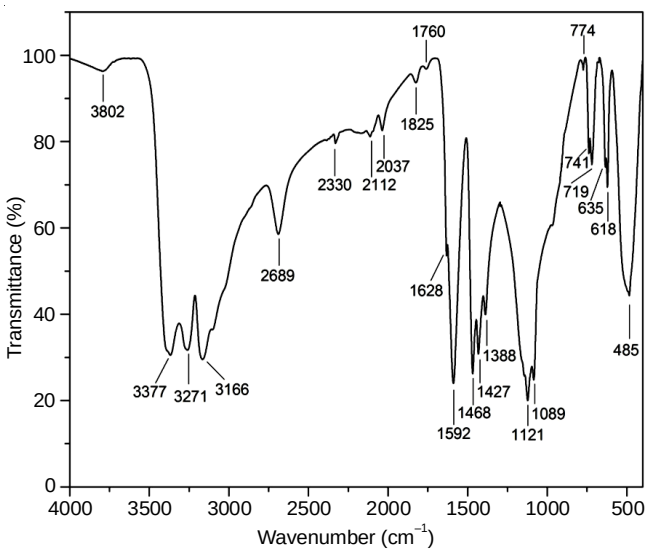

Fig. 3. FT-IR spectrum of BTLSS

TABLE-1
WAVE NUMBER ASSIGNMENT OF BTLSS

Thiourea [Ref. 18]	$Li_2SO_4·H_2O$ [Ref. 19]	Na_2SO_4 [Ref. 20]	BTLSS (**Present work**)	Frequency assignments
3376	–	–	3377	$\gamma_{as}(NH_2)$
3280	–	–	3271	$\gamma_{as}(NH_2)$
3167	–	–	3166	$\gamma_s(NH_2)$
–	2140	2110	2112	γ_2H_2O
–	1638	1636	1628	γ(N–C–N)/$\gamma_s(SO_4)$
1593	–	–	1592	$\delta(NH_2)$
1470	–	–	1468	γ_{as}(C=N)
1414	–	–	1427	γ_{as}(C=S)
–	1125	1097	1121	$\gamma_s(SO_4)$
1089	–	–	1089	γ_s(C=N)
740	–	–	741	γ_s(C=S)
–	–	718	719	$\gamma_s(SO_4)$
648	–	636	635	γ_{as}(N–C–S)
–	615	611	618	$\gamma_s(SO_4)/\delta_s$(N–C–N)
469	479	–	485	γ_s(N–C–S)

γ = Stretching, γ_s = Symmetric stretching, γ_{as} = Asymmetric stretching, δ = bending

Optical studies: For the fabrications of optical devices, particularly NLO, the crystal must be highly transparent for the substantial region of wavelength. The UV-Vis-NIR spectral transmittance spectrum of BTLSS crystal was once recorded in the wavelength range of 190-1100 nm the usage of Perkin Elmer Lamda 35 UV-Vis-NIR spectrometer. From the transmittance spectrum (Fig. 4), it is determined that the lower cutoff wavelength of BTLSS crystal is 300 nm and has a transmittance percentage of 40-55 % in the wavelength range from 350 to 1100 nm. These wide ranges of transparency crystals are well suitable for optoelectronic applications [21].

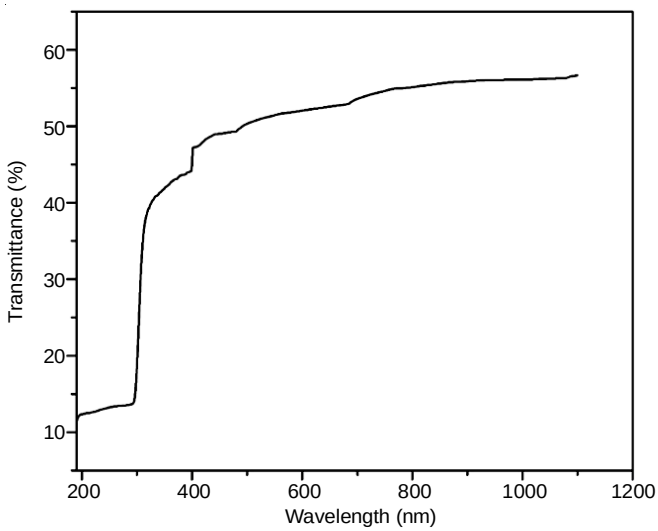

Fig. 4. Optical transmittance spectrum of grown crystal

Determination of optical band gap and extinction coefficient: From measured transmittance, the optical absorption coefficient (α) was derived using the following relation:

$$\alpha = \frac{2.306 \log (1/T)}{t} \quad (1)$$

where 'T' is the transmittance of crystal and't' is the thickness of grown crystal.

The optical band gap (E_g) was evaluated using the following Tauc's relation:

$$\alpha h\nu = A (h\nu - E_g)^{1/2} \quad (2)$$

where 'A' is an arbitrary constant, 'ν' is the frequency of incident photons, 'h' is plank's constant, and E_g is the optical band gap. The value of optical band gap was estimated from the plot of $(\alpha h\nu)^2$ against hν (Fig. 5) and E_g was found to be 3.9 eV.

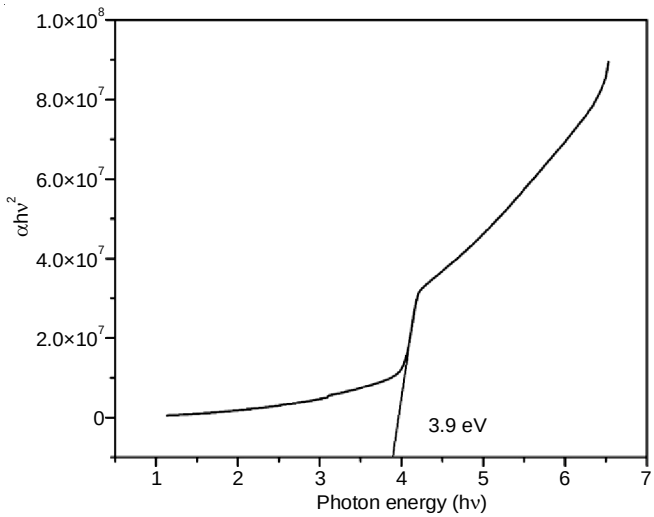

Fig. 5. Optical band gap of BTLSS crystal

The extinction coefficient (k) can be attained from the subsequent equation:

$$K = \frac{\alpha\lambda}{4\pi} \quad (3)$$

The extinction coefficient as a function of photon energy is shown in Fig. 6. The extinction coefficient decreases with energy shows inverse dependence with E up to 4 eV. There is a steep rise in 'k' observed at 4 to 4.25 eV. Again at 4.25 eV there is a decrease of 'k' with energy [22]. Hence, the material is suited for optoelectronic applications.

Photoluminescence: The photoluminescence spectrum was carried out for BTLSS crystal using Carry Eclipse Photoluminescence spectroscopy. The fluorescence spectrum was recorded in the range of 300 to 700 nm with excitation wavelength 280 nm. The single peak observed at 575 nm confirmed

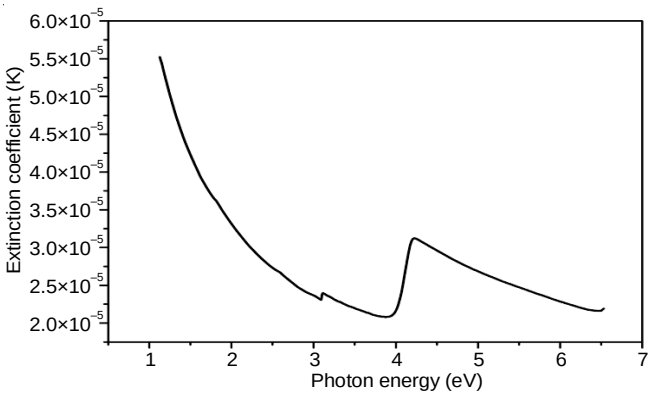

Fig. 6. Photon energy (eV) *vs.* extinction coefficient (k)

the green emission (Fig. 7) by the cause of non-centrosymmetric nature of BTLSS crystal and may be allocated as π-π^* transmission because of interaction between metal (Li^{2+}) and ligand molecule. It illustrated that the purity crystalline nature and NLO property of the grown crystal. From the photoluminescence studies, BTLSS crystal has nonlinear optical properties and verified through Kurtz Perry SHG analysis [23,24].

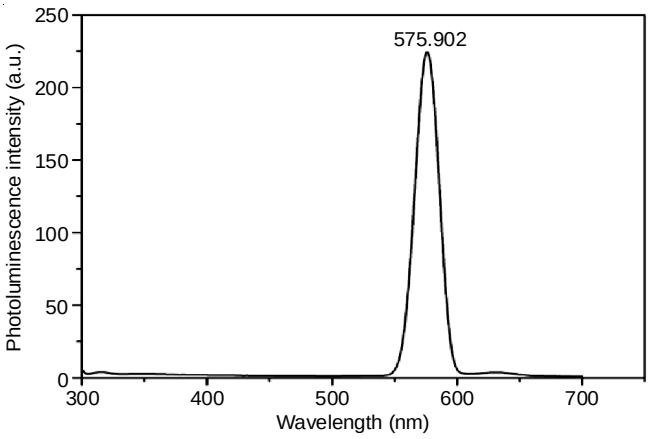

Fig. 7. Photoluminescence spectrum of grown crystal

Second harmonic generation efficiency measurements: The Kurtz and Perry powder technique are most extensively used method for confirming the second harmonic generation from potential second order NLO materials to recognize the materials with non-centrosymmetric crystal structures. The finely powdered forms of BTLSS crystal were carried out the SHG measurement. The prepared powder sample was densely packed in a micro-capillary tube of uniform bore. The beam of a fundamental wavelength at $\lambda = 1064$ nm from a high-intensity Nd:YAG laser (QUANTA RAY Model LAB-170-10/input energy 0.70 J) with 6ns pulse width and a repetition rate of 10 Hz was allowed to fall on the prepared sample. The SHG efficiency of the BTLSS crystal was confirmed by the release of green radiation ($\lambda = 532$ nm) from the sample by the photomultiplier tube. The measured amplitude of second harmonic green light signal of 12.4 mJ was obtained for an input energy of 0.70 J, while the standard potassium dihydrogen orthophosphate (KDP) crystal provided an SHG signal 8.94 mJ for the same input energy. Hence, the relative SHG efficiency is 1.38 times more than that of KDP which demonstrates that BTLSS is a superior NLO material for optoelectronic device fabrication [25,26].

Thermal analysis: Thermogravimetric (TGA) and differential thermal analysis (DTA) of BTLSS crystal was carried out from 30 to 1100 ºC in nitrogen atmosphere at a heating range 30 °C min^{-1} using the instrument NETZSCH STA 449F3. The crystal in powder forms weighting about 33.205 mg used for this investigation [27]. From the TG curve (Fig. 8), the weight losses were observed in five different stages. In the first step, the weight loss starts at 66 ºC and completes at 108 ºC due to the loss of lattice water and the weight loss of about 19 %. Hence, there is no weight loss in the temperature range from 108 to 188 ºC. The remaining steps of gradual mass loss on TG curve are observed between 188 and 714 ºC is due to the liberation of volatile substance like sulfer oxide, nitrogen, carbon, sulphate, *etc*. At this temperature, nearly 48 % of weight is lost. The high mass loss was indicated by the presence of urea in BTLSS. Beyond 714 ºC no significant weight loss noticed and no residue remains. In DTA, the first sharp endothermic peak is indicated at 71.4 ºC (melting point of the substances) and then it undergoes four irreversible endothermic transitions at 110.4, 186.4, 255.4 and 694.4 ºC. The endothermic peaks of DTA trace have coincided well with the decomposition in the TGA trace. The sharpness of endothermic peak demonstrates a good degree of crystallinity and purity.

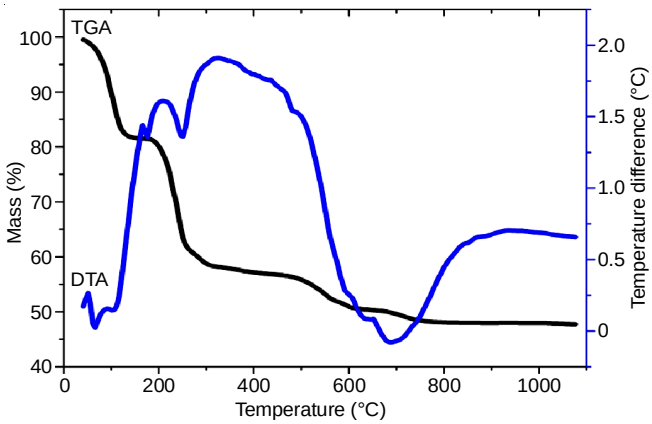

Fig. 8. TGA/DTA curve for grown crystal

Vickers microhardness measurements: The good qualities of single crystals required for device fabrication not only depends on optical behaviours but also on their mechanical performances. The Vickers microhardness test is one of best characterization techniques for studying the mechanical properties of the material, such as cracking yield strength and brittleness index. The transparent BTLSS crystals free from cracks was subjected to the Vickers static indentation test at room temperature (303 K) using a Leitz Wetzler hardness tester fixed with a Vickers diamond pyramidal indenter. The static indentations were made for various loads from 25 to 100 g with a constant indentation time of 5 s for all the loads. The hardness number was evaluated from the relation:

$$H_v = 1.8544 \left(P/d^2\right) \text{ kg/mm}^2 \quad (4)$$

where P is the applied load (g), d is the diagonal length of the impression in (nm) and 1.8544 is a constant. A graph was plotted between log P and log d, which indicates a straight line (Fig. 9). From the graph, BTLSS crystal has a hardness

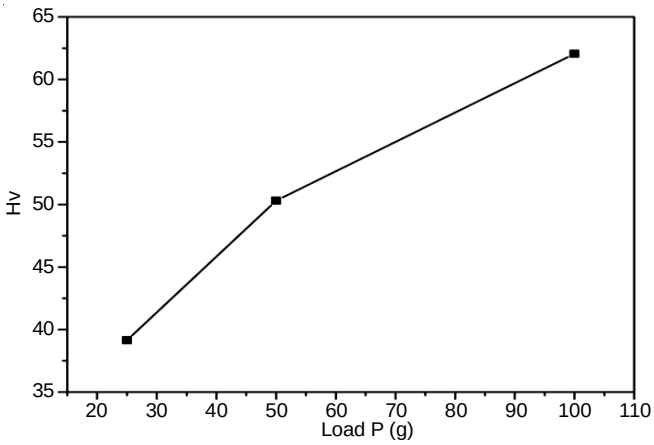

Fig. 9. Hardness behaviour of BTLSS

value of 62.05 kg/mm^2 and the hardness values of grown crystals are increases with increase of applied load up to100 g. If we increase the load above the 100 g, the cracks are started in the crystal [28].

The relation between applied load and diagonal length of indenter is given by Meyer's law :

$$P = ad^n \quad (5)$$

where n is Meyer's index or work hardening exponent and 'a' is an arbitrary constant. Consistent with Onitsch [29] and Hanneman [30], if the values of 'n' lies between 1 and 1.6 it denotes to the hard materials and more than1.6 for soft materials. The graph was obtained between log P and log d which gives a straight line as shown in Fig. 10. From the plot, the work hardening coefficient 'n' was found to be 2.8. It exposes that the material belongs to the soft material category in nature [29-31].

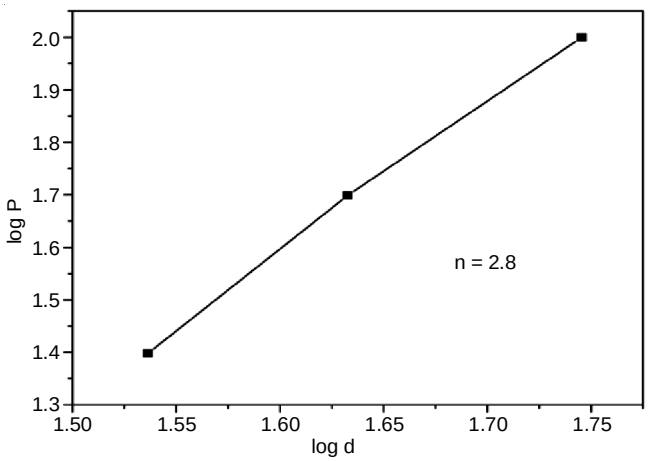

Fig. 10. Meyer's plot of log P *vs.* log d

Vibrating sample magnetometer (VSM) analysis: The magnetic property of grown crystal was analyzed by vibrating sample magnetometer (VSM). To determine the magnetization (magnetic moment per unit volume), the powder sample of BTLSS about 20 mg was located in a glass ampoule mounted in VSM and it was studied by the applied field range 0 to 3 tesla of super conduct magnet at room temperature 303 K. The graph was drawn in between the applied magnetic field (B) and measured magnetization (M). From the plot (Fig. 11), BTLSS crystal exhibited the diamagnetic behaviour [32-34].

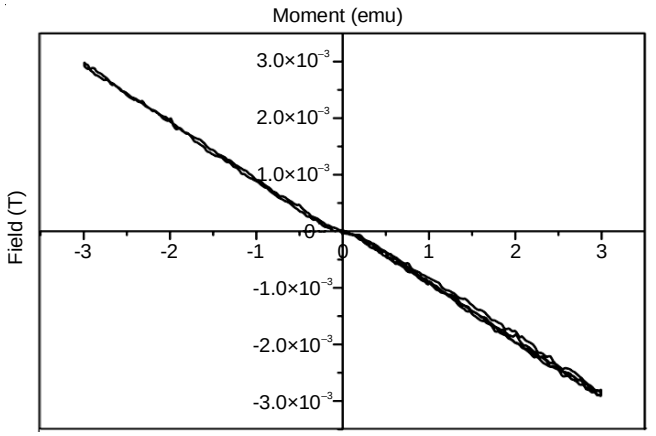

Fig. 11. VSM plot of BTLSS crystal

Conclusion

The good optical quality bisthiorea lithium sodium sulphate (BTLSS) semiorganic single crystal was grown by slow evaporation technique at room temperature. The structural studies of the grown crystal were determined by single crystal X-ray diffraction which expose that orthorhombic structure. The powder X-ray diffraction revealed that BTLSS crystal has good crystallinity and nature. The functional groups of were confirmed by FT-IR spectral analysis. The UV-Vis-NIR spectral analysis revealed that the grown crystal has well transparent in the entire crystal with the lower cut-off wavelength as 300 nm. The optical band gap (E_g) and extinction coefficient (k) was also calculated to determine the optical properties. The luminescence property was exposed as green emission for BTLSS crystal by the photoluminescence spectral analysis. The mechanical strength and work hardening coefficient (n = 2.8) was estimated by Vickers microhardness test. The TGA/DTA analysis is shown the different stages of decomposition and thermal stability of grown crystal. The diamagnetic behaviour of the crystal was studied by VSM analysis. The SHG efficiency was evaluated is 1.38 times than that of potassium dihydrogen orthophosphate (KDP). From these attracting physical, linear and non-linear optical properties concluded that the BTLSS crystal is the suitable candidate for various opto-electronic device applications.

CONFLICT OF INTEREST

The authors declare that there is no conflict of interests regarding the publication of this article.

REFERENCES

1. P.N. Prasad and D.J. Williams, Introduction to Nonlinear Optical Effects in Organic Molecules and Polymers, John Wiley & Sons: New York (1991).
2. H.S. Nalwa and S. Miyata, Nonlinear Optics of Organic Molecules and Polymers, CRC Press: New York (1997).
3. J. Zyss, Molecular Nonlinear Optics: Materials, Physics and Devices, Academic Press: New York (1997).
4. G. Pasupathi, P. Philominathan, *J. Miner. Mater. Charact. Engg.*, **11**, 904 (2012).
5. M.L. Caroline and S. Vasudevan, *Curr. Appl. Phys.*, **9**, 1054 (2009); https://doi.org/10.1016/j.cap.2008.12.001.
6. V. Krishnakumar, C. Ramachandraraja and R.S. Sundararajan, *Spectrochim. Acta A: Mol. Biomol. Spectrosc.*, **68**, 113 (2007); https://doi.org/10.1016/j.saa.2006.09.045.

7. V. Ganesh, M. Shkir, R. Husain, R. Singh, T.B. Rao and K.K. Rao, *Optik*, **124**, 6690 (2013); https://doi.org/10.1016/j.ijleo.2013.05.087.
8. S. Sagadevan, *Optik*, **125**, 6746 (2014); https://doi.org/10.1016/j.ijleo.2014.08.059.
9. M. Selvapandiyan, J. Arumugam, P. Sundaramoorthi and S. Sudhakar, *J. Alloys Compd.*, **580**, 270 (2013); https://doi.org/10.1016/j.jallcom.2013.05.071.
10. S. Selvakumar, S.M.R. Kumar, G.P. Joseph, K. Rajarajan, J. Madhavan, S.A. Rajasekar and P. Sagayaraj, *Mater. Chem. Phys.*, **103**, 153 (2007); https://doi.org/10.1016/j.matchemphys.2007.02.005.
11. R. Hanumantharao and S. Kalainathan, *J. Phys. Chem. Solids*, **73**, 724 (2012); https://doi.org/10.1016/j.jpcs.2012.01.011.
12. G. Ramasamy and S. Meenakshisundaram, *J. Cryst. Growth*, **377**, 197 (2013); https://doi.org/10.1016/j.jcrysgro.2013.05.021.
13. N. Bhuvaneswari, K. Baskar and R. Dhanasekaran, *Optik*, **126**, 3731 (2015); https://doi.org/10.1016/j.ijleo.2015.08.246.
14. K. Uma, R. Manimekalai and G. Pasupathi, *Int. J. Chem. Mater. Res.*, **3**, 91 (2015); https://doi.org/10.18488/journal.64/2015.3.4/64.4.91.99.
15. K. Murugadoss, K. Gayathiridevi and G. Pasupathi, *J. Opt.*, **45**, 136 (2016); https://doi.org/10.1007/s12596-015-0301-6.
16. K. Nakamoto, Infrared and Raman Spectra of Inorganic and Coordination Compounds, Wiley: New York (1986).
17. G. Pasupathi and P. Philominathan, *Mater. Lett.*, **62**, 4386 (2008); https://doi.org/10.1016/j.matlet.2008.07.023.
18. S. Selvakumar, S.M.R. Kumar, K. Rajarajan, A.J.A. Pragasam, S.A. Rajasekar, K. Thamizharasan and P. Sagayaraj, *Cryst. Growth Des.*, **6**, 2607 (2006); https://doi.org/10.1021/cg060414p.
19. R. Priya, S. Krishnan, C.J. Raj and S.J. Das, *Cryst. Res. Technol.*, **44**, 1272 (2009); https://doi.org/10.1002/crat.200900504.
20. A. Periyasamy, S. Murugan and M. Palaniswamy, *Rasayan J. Chem.*, **4**, 981 (2009).
21. S. Suresh, *Optik*, **125**, 1223 (2014); https://doi.org/10.1016/j.ijleo.2013.07.154.
22. R.H. Rao and S. Kalainathan, *Spectrochim. Acta A: Mol. Biomol. Spectrosc.*, **97**, 456 (2012); https://doi.org/10.1016/j.saa.2012.06.033.
23. K.T Rathod, I.B. Patel, C.F. Desai, Y.H. Gandhi, *Int. J. Lumin. Appl.*, **5**, 86 (2015).
24. S. Ariponnammal, S. Chandrasekaran and C. Sanjeeviraja, *Dig. J. Nanomater. Biostruct.*, **7**, 947 (2012).
25. S.K. Kurtz and T.T. Perry, *J. Appl. Phys.*, **39**, 3798 (1968); https://doi.org/10.1063/1.1656857.
26. K. Kiguchi, M. Kato, M. Okunaka and Y. Taniguchi, *Appl. Phys. Lett.*, **60**, 1933 (1992); https://doi.org/10.1063/1.107155.
27. J. Ramajothi, S. Dhanuskodi and K. Nagarajan, *Cryst. Res. Technol.*, **39**, 414 (2004); https://doi.org/10.1002/crat.200310204.
28. B.W. Mott, Micro-Indentation Hardness Testing, Buterworths: London (1956).
29. E.M. Onitch, *Mikroscopie*, **2**, 131 (1947).
30. M. Hanneman, *Metallurgia Manchu.*, **23**, 135 (1941).
31. K.K. Rao and D.B. Sirdeshmukh, *Bull. Mater. Sci.*, **5**, 449 (1983); https://doi.org/10.1007/BF02743923.
32. S. Karthick, A.A. Irudayaraj, A.D. Raj and R. Vinayagamoorthy, *Int. J. Technol. Res. Appl.*, **37**, 86 (2016).
33. P. Maadeswaran, S. Thirumalairajan and J. Chandrasekaran, *Optoelectron. Adv. Mater.*, **3**, 36 (2009).
34. G. Pasupathi, K. Uma, C. Ramachandra Raja and R. Manimekalai, *Mater. Lett.*, **161**, 224 (2015); https://doi.org/10.1016/j.matlet.2015.07.111.